HHS Public Access

Author manuscript

Am J Surg Pathol. Author manuscript; available in PMC 2019 August 08.

Published in final edited form as:

Am J Surg Pathol. 2019 January ; 43(1): 121–131. doi:10.1097/PAS.0000000000001170.

Somatic Mutations of *TSC2* or *MTOR* Characterize a Morphologically Distinct Subset of Sporadic Renal Cell Carcinoma with Eosinophilic and Vacuolated Cytoplasm

Ying-Bei Chen, MD, PhD[1,*], **Leili Mirsadraei, MD**[1], **Gowtham Jayakumaran, MS**[1], **Hikmat A. Al-Ahmadie, MD**[1], **Samson W. Fine, MD**[1], **Anuradha Gopalan, MD**[1], **S. Joseph Sirintrapun, MD**[1], **Satish K. Tickoo, MD**[1], **Victor E. Reuter, MD**[1]

[1]Department of Pathology, Memorial Sloan Kettering Cancer Center, New York, NY, USA

Abstract

The differential diagnosis of renal cell neoplasms with solid or nested architecture and eosinophilic cytoplasm has become increasingly complex. Despite recent advances in classifying a number of entities exhibiting this morphology, some tumors remain in the unclassified category. Here we describe a morphologically distinct group of sporadic renal cell carcinoma (RCC) with predominantly nested architecture, eosinophilic and remarkably vacuolated cytoplasm retrospectively identified from a cohort of previously unclassified tumors. We examined the clinicopathologic and immunohistochemical features of these tumors and investigated their mutational and copy number alterations using a targeted next-generation sequencing (NGS) platform. The study included 7 patients with a mean age of 54 years (range 40–68) and a male to female ratio of 3:4. All patients presented with a solitary renal mass and had no prior medical or family history raising concern for syndromic conditions. Tumors were well-circumscribed, unencapsulated, and comprised of nests of eosinophilic cells in a hypocellular and often edematous stroma. Tumor cells had round nuclei with prominent nucleoli and granular cytoplasm with striking vacuolization. Thick-walled vessels and calcifications were also frequently present, whereas increased mitotic activity, necrosis, foamy histiocytes or lymphocytic infiltrates were not identified. All cases were positive for PAX8, had retained expression of SDHB and FH, and exhibited a CK7(−)/CK20(−) phenotype. While cathepsin-K was positive in 5 cases, none exhibited immunoreactivity to HMB45 or Melan A, or TFE3 immunostaining. NGS identified somatic inactivating mutations of *TSC2* (3 of 5 tumors tested) or activating mutations of *MTOR* (2 of 5) as the primary molecular alterations, consistent with hyperactive mTOR complex 1 (mTORC1) signaling which was further demonstrated by phospho-S6 and phospho-4E-BP1 immunostaining. Copy number analysis revealed a loss of chromosome 1 in both cases with *MTOR* mutation. These tumors represent a novel subset of sporadic RCC characterized by alterations in TSC1-TSC2 complex or the mTORC1 pathway. Recognition of their characteristic morphologic and immunophenotypic features will allow them to be readily identified and separated from the unclassified RCC category.

[*]Corresponding Author: Ying-Bei Chen, MD, PhD, Assistant Attending Pathologist, Department of Pathology, Memorial Sloan Kettering Cancer Center, New York, NY 10065, Tel: (212) 639-6338, Fax: (212) 717-3203, cheny@mskcc.org.

Disclosures: The authors have no conflicts of interest to disclose.

Keywords

sporadic renal cell carcinoma; TSC; MTOR; somatic mutations

Introduction

The differential diagnosis of renal cell tumors with mainly nested, tubular or solid architecture and eosinophilic cytoplasm has expanded in recent years. Depending on the tumor histomorphology and findings from the adjacent renal parenchyma, beyond common histologic subtypes such as oncocytoma or eosinophilic variant of chromophobe renal cell carcinoma (chRCC), consideration now may include tumors occurring in patients with Birt-Hogg-Dubé (BHD) syndrome,[1, 2] renal oncocytosis,[3] or tuberous sclerosis complex (TSC),[4, 5] SDH-deficient renal cell carcinoma (RCC),[6] fumarate hydratase (FH)-deficient RCC,[7, 8] MiT family (*TFE3* or *TFEB*) translocation RCC,[9] as well as unclassified RCC. Moreover, an entity termed eosinophilic solid and cystic (ESC) RCC has recently been described as a sporadic form of RCC with histologic similarity to a subset of renal tumors encountered in TSC patients.[10, 11] While the molecular alterations in ESC RCC are still under active investigation, emerging evidence shows that some of these tumors are characterized by somatic *TSC2* or *TSC1* mutations.[12–14]

Tumor suppressor *TSC1* and *TSC2* genes are essential negative regulators of the mammalian target of rapamycin (mTOR) complex 1 (mTORC1) signaling. The proteins they encode, hamartin and tuberin respectively, interact and form a heterodimer that inhibits the activation of mTORC1, a master regulator of nutrient and growth-factor-induced signaling.[15, 16] In RCC, mTOR inhibitors represent an important therapeutic approach for advanced disease.[17] Interestingly, while inactivating mutations of *TSC1*/*TSC2* or activating mutations of *MTOR* occur in the common subtypes of RCC, their reported frequencies are typically low (e.g. *TSC1*/*TSC2* at about 1–3%, *MTOR* 3–5%) and often co-occur with other characteristic molecular alterations of the corresponding histologic subtype.[18–20] Although believed to be an important pathway implicated in the pathogenesis of RCC, it remains unclear whether these mutations alone drive the development of renal cell tumors in sporadic settings.

We have previously described a subset of high-grade unclassified RCC (uRCC) characterized by mutually exclusive mutations in *TSC1*, *TSC2*, *MTOR* or *PTEN* and hyperactive mTORC1 signaling.[21] For a few of these tumors particularly, *TSC1*, *TSC2* or *MTOR* somatic mutation was the only molecular alteration detected among the 230 cancer-related genes investigated by a targeted next-generation sequencing (NGS) panel, suggesting them as the driver of the tumor development.

In the current study, we characterized a morphologically distinct group of RCC that occurred in sporadic settings and displayed predominantly nested architecture, eosinophilic and remarkably vacuolated cytoplasm. We examined the clinicopathologic and immunohistochemical features of these tumors and investigated their mutational and copy number alterations using a targeted NGS platform.

Materials and methods

Case selection and histologic review

The study included 7 retrospectively identified cases with similar histomorphology. All 7 cases were initially diagnosed as “RCC, unclassified”, 4 of which were from patients who underwent nephrectomy at our institution and 3 were from the consultation files of one of the authors. One index case was previously included in a molecular analysis study of uRCC.[21] All archival material from these cases was retrieved and re-reviewed. All available clinical data were obtained through chart review (n=5) or provided by the outside submitting physicians (n=2). Results of pre-operative imaging studies were available for review in 6 of 7 cases. The 8th edition AJCC TNM system was used for tumor staging. The study was approved by our Institutional Review Board.

Immunohistochemistry

Immunohistochemistry was conducted using 5 μm formalin-fixed paraffin-embedded (FFPE) whole tissue sections. Staining for common markers including Pax8 (Proteintech, 1:100), CK7 (OV-TL 12/30, DAKO, 1:800), CK20 (Ks20.8, DAKO, 1:1600), CD117 (Cat# A4502, DAKO, 1:1000), TFE3 (MRQ37, Cell Marque), HMB45 (HMB45, DAKO, 1:100), and Melan A (A103, Ventana) was performed using a BenchMark automated system (Roche). Staining for cathepsin-K (3F9, ABCAM, 1:5000) and FH (J13, Santa Cruz, 1:2500) was accomplished using a Bond III automated system (Leica). Staining for SDHB (21A11, Abcam, 1: 100), phospho-S6 (Ser235/236) (D57.2.2E, Cell Signaling Technology, 1:100), and phospho-4E-BP1 (Thr37/46) (236B4, Cell Signaling Technology, 1:400) was performed using an automated Ventana Discovery system (Roche). For CK7 and CK20 staining, the result was interpreted as “negative” if no or rare (<5%) cells staining positive. Immunostaining scores (H-scores) for phospho-S6 and phospho-4E-BP1 were determined as [H= intensity (0–3) x percentage of positive cells (1–100)].

Molecular analysis

All H&E slides were reviewed to select representative areas of the tumors and normal tissues for the molecular analysis. The corresponding areas from unstained FFPE tissue sections were macro-dissected for DNA extraction using QIAamp DNA FFPE tissue kit according to the manufacturer’s standard protocol (Qiagen). Among the 5 cases with molecular analysis, 3 had paired tumor and normal DNA samples, and 2 had only tumor DNA available.

DNA samples were subjected to MSK-IMPACT, a hybridization capture-based NGS assay for targeted deep sequencing of all exons and selected introns of key cancer genes.[22] Aside from case 1, which was analyzed using an early version of the platform (230 genes),[21] all other cases were analyzed for alterations in ≥ 410 genes (Supplementary Table 1). In cases with paired tumor and normal samples, somatic mutations were called after private germline SNVs detected in the paired normal sample were appropriately filtered out. The functional impacts of detected mutations were categorized as oncogenic/likely oncogenic and variants of unknown significance (VUS) using OncoKB (http://oncokb.org), a precision oncology knowledge base maintained at MSKCC.[23] The NGS data were also analyzed by FACETS,

an allele-specific copy number analysis tool, for the detection of loss, gain, amplification or copy-neutral loss of heterozygosity (CN-LOH).[24]

Results

Clinical features

The clinical characteristics of these 7 cases are summarized in Table 1. The mean age at presentation was 54 years (range, 40 to 68 y) with a male to female ratio of 3:4. Tumor size ranged from 1.5 to 5 cm (mean 3.4 cm). All patients presented with a solitary renal mass incidentally detected during clinical workup for urinary tract symptoms/infection, trauma, or health screening. Except for one patient with a concurrent 2.3 cm simple cyst, available imaging results from 6 of 7 patients were negative for other lesions in the ipsilateral and contralateral kidneys. No patients had prior medical history raising concern for TSC, or family history of renal cancer or any syndromic conditions. All patients underwent partial nephrectomy and were found to have localized disease. All 5 patients with clinical follow-up data had no evidence of disease at the last visit. The median follow-up time was 14 months.

Pathologic features

Grossly, tumors were well-circumscribed with tan-yellow to tan-brown, soft, and slightly heterogeneous cut surfaces. The tumors were mostly solid, and some appeared to have grossly visible intratumoral medium to large caliber vessels (Fig. 1A).

Microscopically, all these 7 tumors shared similar morphologic features. All 7 were predominantly composed of nests of eosinophilic cells in a hypocellular and often edematous stroma (Fig. 1B–C). However, in each tumor, a variable number of cells were also arranged as dispersed single cells or in minute clusters (Fig. 1C). There were thick-walled vessels scattered within or at the periphery of the tumors, consistent with the gross findings (Fig. 1B–C). The tumor cells exhibited round nuclei with conspicuous, large nucleoli and abundant, eosinophilic and granular cytoplasm. The cytoplasm often showed striking vacuolization (Fig. 1D–F). These cytoplasmic vacuoles varied in size and frequently coalesced into a large space, displacing the nucleus to the periphery of the cell. The tumor cells also varied considerably in size, but large cells with abundant cytoplasm predominated. The basement membrane-like material around tumor nests and the membranes of large cytoplasmic vacuoles often had accentuated eosinophilic staining, imparting a plant cell-like appearance to some tumor cells. Multinucleated tumor cells were present. However, given the extreme vacuolization, it was sometimes difficult to discern multinucleation from multiple tumor cells within tumor nests (Fig. 1F). There were no apparent mitoses found despite the high nuclear grade. Necrosis was also absent. No foamy histiocytes or lymphocytic infiltrates were identified in the stroma.

The tumors were unencapsulated, and entrapped renal tubules were frequently found at the periphery or occasionally deeply within the tumor (Fig. 2A). Calcifications were found in 4 cases: one case exhibited extensive calcification of tumor nests (Fig. 2B), stroma and intratumoral vessels; 3 other tumors had scattered microcalcifications (Fig. 2C). In focal areas where cytoplasmic vacuolization was less prominent, perinuclear clearing could be

seen (Fig. 2C). While this might raise suspicion for chRCC, nuclear contours remained smooth throughout, even in these areas. Some tumor cells displayed cytoplasmic filamentous material and/or stippling (Fig. 2D). In areas with tightly packed nests, the marked vacuolization occasionally imparted a cribriform or sieve-like appearance (Fig. 2E). Additionally, an abrupt transition could be seen between tumor cells showing prominent vacuolization and tumor cells with dense, granular cytoplasm (Fig. 2F). The adjacent renal parenchyma available for histologic assessment was unremarkable in 6 cases, and the remaining one showed mild arteriosclerosis changes.

Immunohistochemical features

The immunohistochemical features of the 7 cases (Fig. 3) are summarized in Table 2. All cases were positive for PAX8 and showed retained expression of SDHB and FH. The CK7 and CK20 stains were essentially negative, with at most rare cells or vacuoles showing positive staining (Fig. 3B–C). CD117 displayed a weak, membranous staining pattern in 4 of 7 cases, (Fig. 3D), while being negative in the other 3. Interestingly, cathepsin-K was positive in 5 cases, including 4 showing relatively diffuse, membranous staining (Fig. 3E). The tumors were negative for HMB45, Melan A, and TFE3 immunostaining. The tumor cells were positive for pan-cytokeratin (AE1/AE3), EMA, and CD10, while being negative for CA-IX in 3 cases where these stains were performed. Two cases analyzed by *TFEB* break-apart fluorescence in-situ hybridization (FISH) assay were both negative for the gene rearrangement.

Molecular analysis

Among 5 cases with molecular analysis data (Table 2), 3 showed somatic *TSC2* inactivating mutations, including 2 cases harboring two independent *TSC2* mutations, likely representing biallelic inactivation. The other 2 cases had *MTOR* p.L2427R mutation, a mutation we have previously demonstrated to be an activating mutation that leads to hyperactive mTORC1 signaling.[21] The somatic nature of these mutations and a lack of germline alterations in *TSC1* and *TSC2* genes were further confirmed by independent clinical genetic analysis in cases 1, 2, and 4, whereas the variant allele frequencies of detected *MTOR* or *TSC2* mutations in the two cases without paired normal DNA samples (cases 5 and 6) were also consistent with somatic mutations. In these two latter cases, rare additional mutations with unknown significance (VUS in Table 2) were found, but neither was recurrent.

In line with the finding that these tumors harbored somatic *TSC2* inactivating mutations or *MTOR* activating mutations, all 6 cases tested for phospho-S6 (p-S6) and phospho-4E-BP1(p-4EBP1) by immunohistochemistry showed diffuse, strong staining (Fig. 4 and Table 2), consistent with the presence of hyperactive mTORC1 signaling.

While there were no consistent copy number alterations detected in 4 cases analyzed by FACETS, both cases with *MTOR* (1p36.22) activating mutations harbored a loss of chromosome 1 (Fig. 5). None of the cases showed characteristic copy number alterations associated with the usual histologic subtypes of RCC, nor exhibited gains of 7 and 16, the most frequent copy number alterations recently described for ESC RCC.[10]

Discussion

In this study, we describe a morphologically distinctive group of sporadic RCC with nested, eosinophilic cells showing extreme cytoplasmic vacuolation. We further demonstrate that these tumors are characterized by somatic mutations of *TSC2* or *MTOR* that lead to hyperactive mTORC1 signaling.

The relatively unique histomorphology we observed in this group of tumors does not fit into any of the established histologic subtypes of RCC. Compared to other entities that are in the differential diagnosis of renal tumors with nested or solid architecture and eosinophilic cells, these cases exhibited an architectural resemblance to oncocytoma at low-power magnification, with predominantly solid nests of neoplastic cells in a hypocellular stroma with hyalinization or edematous changes. However, the marked variations in tumor cell size and shape, as well as the nuclear pleomorphism are unquestionably beyond what can be accepted for oncocytoma. While the nuclear pleomorphism and cytoplasmic clearing might raise concerns for chRCC, they lacked the typical nuclear membrane irregularity ("raisinoid" nuclei) seen in chRCC. The presence of prominent cytoplasmic vacuolization rather than perinuclear clearing is another distinguishing feature. The cytoplasmic eosinophilia, striking vacuolization, and thick-walled vessels would also lead to a consideration of epithelioid angiomyolipoma, adrenal cortical neoplasm, TFE3 or TFEB-translocation RCC, SDH-deficient or FH-deficient RCC. These possibilities were excluded by ancillary studies: the tumors were positive for PAX8 and Pan-CK, while being negative for TFE3, HMB45, or Melan A; they had retained SDHB and FH immunoreactivity and were negative for *TFEB* fusion by FISH. However, the immunoreactivity to cathepsin-K and weak staining for CD117 in some cases could be misleading, emphasizing the need to perform a panel of immunostains to address the differential diagnosis of RCC with unusual features.

The histomorphology of these tumors is also different from the renal tumors that have been described in BHD or renal oncocytosis patients. Additionally, all the patients presented with solitary renal mass and lacked radiographic or histologic changes in the adjacent renal parenchyma suggestive of RCC-related syndromic conditions or acquired cystic disease (ACD)-associated RCC. Nonetheless, it is interesting to note that rare cases from previous studies of TSC-associated RCC appeared to show nested eosinophilic cells with marked cytoplasmic vacuolization (e.g. Fig. 1E in Schreiner et al,[25] Fig. 6H in Yang et al,[5] and Fig. 3E in Guo et al[4]), however, it is difficult to be certain whether these few TSC-associated RCC are morphologically and immunophenotypically similar to the cases in our study based on the available information.

It is also interesting to compare the clinicopathologic features of this subset of tumors in our study to the recently described ESC RCC, a sporadic form of RCC with morphologic similarity to a subset of renal tumors occurring in patients with TSC. As reported by Trpkov et al,[10, 11] some ESC RCC may also show marked intracytoplasmic vacuolization, nested architecture, cell size variations, etc., but a few morphologic features that have been stressed for the ESC RCC were not seen in this group of RCC. First, ESC RCC typically shows solid and cystic architecture, with a confluent growth of sheets or less commonly nests of tumor cells with almost invariably admixed small aggregates of histiocytes and lymphocytes. In

contrast, our cases were predominantly nested, showed dispersed single or minute clusters of tumor cells, and completely lacked admixed aggregates of histiocytes or lymphocytes. Second, ESC RCC exhibits a predominant CK20(+)/CK7(−) immunophenotype, whereas our cases were all CK20(−)/CK7(−). Only rare cells or occasional large vacuoles showed some staining for both CK7 and CK20, the frequency of which for CK20 was well below the 5% cut-off value used by the ESC RCC studies to define positivity. Third, ESC RCC occurs predominantly in women, while our cases included both male and female patients (M:F=3:4), although it is interesting to note that in a cohort of 10 ESC RCC cases reported in young patients, there were 4 male patients.[8] Another recently reported cohort of 7 molecularly characterized cases also included one male.[13]

Molecularly, we demonstrate that the tumors in this study harbor *TSC2* or *MTOR* somatic mutations. These were the only recurrent molecular alterations detected by a targeted NGS panel that interrogates more than 400 key cancer genes, including a vast majority of those implicated in the pathogenesis of RCC. Not only were the clinical presentations of these patients not suspicious for hereditary RCC conditions, the NGS sequencing data and independent germline testing further supported the somatic nature of these mutations. The detection of two independent inactivating mutations of the *TSC2* gene also suggests biallelic inactivation of this tumor suppressor gene. Meanwhile, *MTOR* p.L2427R is the same recurrent activating mutation that we have previously identified in 3 high-grade uRCC cases with hyperactive mTORC1 signaling.[21] The concurrent loss of chromosome 1 in both cases with *MTOR* mutation also suggests that the wildtype *MTOR* gene (located at 1p36.22) is likely lost in these tumors. Consistent with their regulatory roles in the mTORC1 pathway, the tumors in our study with either *TSC2* inactivating mutations or *MTOR* activating mutation displayed strong staining for both p-S6 and p-4EBP1, supporting the presence of a hyperactive mTORC1 signaling. We did not identify histologic differences between cases with mutations in *TSC2* vs. those with *MTOR* mutations in this small cohort.

Importantly, the copy number alterations we detected in this group of tumors do not show specific patterns suggestive of any established histologic subtypes, and they also appear to be distinct from the frequent copy number alterations reported in ESC RCC.[10] Taken together, the molecular evidence strongly supports this histologically distinguishable group of renal tumors described in the current study as a molecularly distinct form of sporadic RCC driven by the mutated *TSC2* or *MTOR* genes, which should be recognized and separated from uRCC cases.

Given the diverse morphologic spectrum observed in TSC-associated RCC,[4, 5] it is tempting to speculate that their sporadic counterparts may also show a spectrum of histomorphology. This hypothesis is supported by evidence linking ESC RCC to somatic mutations of *TSC2* or *TSC1* genes,[12–14] whereas our current study identifies a morphologically distinct group of RCC harboring *TSC2* or *MTOR* somatic mutations as the primary molecular alterations. However, the recently reported series of ESC RCC have included cases with unusual features, including rare cases exhibiting prominent cytoplasmic vacuolization.[10, 14] Further experience and studies with molecular analysis apparently are needed to determine the relationship between tumors we described and ESC RCC, as well as to clarify the pathologic spectrum of sporadic RCC primarily driven by *TSC1/TSC2* or *MTOR* alterations.

Interestingly, the molecular analysis we conducted in this study suggests that activating mutation of *MTOR* gene can lead to similar tumor phenotype as biallelic *TSC2* inactivating mutations.

All 7 cases in the current cohort were organ-confined, and there was no evidence of recurrence or progression after surgical removal. However, given the relatively short follow-up time, the biologic behavior of this group remains unclear. In comparison, while the majority of reported ESC RCC cases have indolent behavior, a few cases with metastasis have been reported very recently.[8, 26, 27]

In our previously described molecular subset of uRCC with hyperactive mTORC1 signaling, aside from the index case included in the current study, there were a few other cases comprised of solid sheets/nests of high-grade eosinophilic cells with focal cytoplasmic vacuolization and harboring biallelic *TSC2* or activating *MTOR* mutations.[21] However, these few cases had other concurrent molecular alterations such as mutations in other cancer-related genes including *ATM* or *KMT2C*, and exhibited histologic features beyond what have been described for TSC-associated RCC and ESC RCC; nor did these have the consistent histologic findings we observed in the current cohort of 7 cases (unpublished data). We believe further studies are needed to determine the best classification of these few additional uRCC cases with hyperactive mTORC1 signaling.

In summary, we describe a morphologically distinctive group of sporadic RCC with eosinophilic and markedly vacuolated cytoplasm, nested architecture with dispersed single or minute clusters of tumor cells, and frequent calcifications. Molecularly, these tumors are characterized by somatic mutations of *TSC2* or *MTOR* genes and hyperactive mTORC1 signaling. Although rare, we believe these tumors represent a novel subset of sporadic RCC in which alterations in TSC1-TSC2 complex or the mTORC1 are the primary driving force for tumor development. Their characteristic morphologic and immunophenotypic features allow them to readily recognized and separated from the uRCC category.

Supplementary Material

Refer to Web version on PubMed Central for supplementary material.

Acknowledgments

Source of Funding: Supported in part by the NIH/NCI Cancer Center Support Grant (P30 CA008748) and The Society of Memorial Sloan Kettering Research Grant (Y-B.C.).

References

1. Pavlovich CP, Walther MM, Eyler RA, et al. Renal tumors in the Birt-Hogg-Dube syndrome. Am J Surg Pathol. 2002;26:1542–1552. [PubMed: 12459621]
2. Furuya M, Yao M, Tanaka R, et al. Genetic, epidemiologic and clinicopathologic studies of Japanese Asian patients with Birt-Hogg-Dube syndrome. Clin Genet. 2016;90:403–412. [PubMed: 27220747]
3. Tickoo SK, Reuter VE, Amin MB, et al. Renal oncocytosis: a morphologic study of fourteen cases. Am J Surg Pathol. 1999;23:1094–1101. [PubMed: 10478670]

4. Guo J, Tretiakova MS, Troxell ML, et al. Tuberous sclerosis-associated renal cell carcinoma: a clinicopathologic study of 57 separate carcinomas in 18 patients. Am J Surg Pathol. 2014;38:1457–1467. [PubMed: 25093518]
5. Yang P, Cornejo KM, Sadow PM, et al. Renal cell carcinoma in tuberous sclerosis complex. Am J Surg Pathol. 2014;38:895–909. [PubMed: 24832166]
6. Gill AJ, Hes O, Papathomas T, et al. Succinate dehydrogenase (SDH)-deficient renal carcinoma: a morphologically distinct entity: a clinicopathologic series of 36 tumors from 27 patients. Am J Surg Pathol. 2014;38:1588–1602. [PubMed: 25025441]
7. Smith SC, Sirohi D, Ohe C, et al. A distinctive, low-grade oncocytic fumarate hydratase-deficient renal cell carcinoma, morphologically reminiscent of succinate dehydrogenase-deficient renal cell carcinoma. Histopathology. 2017;71:42–52. [PubMed: 28165631]
8. Li Y, Reuter VE, Matoso A, et al. Re-evaluation of 33 'unclassified' eosinophilic renal cell carcinomas in young patients. Histopathology. 2018;72:588–600. [PubMed: 28898443]
9. Argani P MiT family translocation renal cell carcinoma. Semin Diagn Pathol. 2015;32:103–113. [PubMed: 25758327]
10. Trpkov K, Abou-Ouf H, Hes O, et al. Eosinophilic Solid and Cystic Renal Cell Carcinoma (ESC RCC): Further Morphologic and Molecular Characterization of ESC RCC as a Distinct Entity. Am J Surg Pathol. 2017;41:1299–1308. [PubMed: 28786877]
11. Trpkov K, Hes O, Bonert M, et al. Eosinophilic, Solid, and Cystic Renal Cell Carcinoma: Clinicopathologic Study of 16 Unique, Sporadic Neoplasms Occurring in Women. Am J Surg Pathol. 2016;40:60–71. [PubMed: 26414221]
12. Parilla M, Kadri S, Patil SA, et al. Are Sporadic Eosinophilic Solid and Cystic Renal Cell Carcinomas Characterized by Somatic Tuberous Sclerosis Gene Mutations? The American Journal of Surgical Pathology. 9000;Publish Ahead of Print.
13. Mehra R, Vats P, Cao X, et al. Somatic Bi-allelic Loss of TSC Genes in Eosinophilic Solid and Cystic Renal Cell Carcinoma. Eur Urol. 2018;74:483–486. [PubMed: 29941307]
14. Palsgrove DN, Li Y, Pratilas CA, et al. Eosinophilic Solid and Cystic (ESC) Renal Cell Carcinomas Harbor TSC Mutations: Molecular Analysis Supports an Expanding Clinicopathologic Spectrum. Am J Surg Pathol. 2018;42:1166–1181. [PubMed: 29975249]
15. Laplante M, Sabatini DM. mTOR signaling in growth control and disease. Cell. 2012;149:274–293. [PubMed: 22500797]
16. Dibble CC, Manning BD. Signal integration by mTORC1 coordinates nutrient input with biosynthetic output. Nat Cell Biol. 2013;15:555–564. [PubMed: 23728461]
17. Choueiri TK, Motzer RJ. Systemic Therapy for Metastatic Renal-Cell Carcinoma. N Engl J Med. 2017;376:354–366. [PubMed: 28121507]
18. The Cancer Genome Atlas Research Network. Comprehensive molecular characterization of clear cell renal cell carcinoma. Nature. 2013;499:43–49. [PubMed: 23792563]
19. The Cancer Genome Atlas Research Network, Linehan WM, Spellman PT, et al. Comprehensive Molecular Characterization of Papillary Renal-Cell Carcinoma. N Engl J Med. 2016;374:135–145. [PubMed: 26536169]
20. Davis CF, Ricketts CJ, Wang M, et al. The somatic genomic landscape of chromophobe renal cell carcinoma. Cancer Cell. 2014;26:319–330. [PubMed: 25155756]
21. Chen YB, Xu J, Skanderup AJ, et al. Molecular analysis of aggressive renal cell carcinoma with unclassified histology reveals distinct subsets. Nat Commun. 2016;7:13131. [PubMed: 27713405]
22. Cheng DT, Mitchell TN, Zehir A, et al. Memorial Sloan Kettering-Integrated Mutation Profiling of Actionable Cancer Targets (MSK-IMPACT): A Hybridization Capture-Based Next-Generation Sequencing Clinical Assay for Solid Tumor Molecular Oncology. J Mol Diagn. 2015;17:251–264. [PubMed: 25801821]
23. Chakravarty D, Gao J, Phillips SM, et al. OncoKB: A Precision Oncology Knowledge Base. JCO precision oncology. 2017;1:1–11.
24. Shen R, Seshan VE. FACETS: allele-specific copy number and clonal heterogeneity analysis tool for high-throughput DNA sequencing. Nucleic Acids Res. 2016;44:e131. [PubMed: 27270079]
25. Schreiner A, Daneshmand S, Bayne A, et al. Distinctive morphology of renal cell carcinomas in tuberous sclerosis. Int J Surg Pathol. 2010;18:409–418. [PubMed: 19403547]

26. McKenney JK, Przybycin CG, Trpkov K, et al. Eosinophilic solid and cystic renal cell carcinomas have metastatic potential. Histopathology. 2018;72:1066–1067. [PubMed: 29265482]

27. Tretiakova MS. Eosinophilic solid and cystic renal cell carcinoma mimicking epithelioid Angiomyolipoma: series of 4 primary tumors and 2 metastases. Hum Pathol. 2018;80:65–75. [PubMed: 29885406]

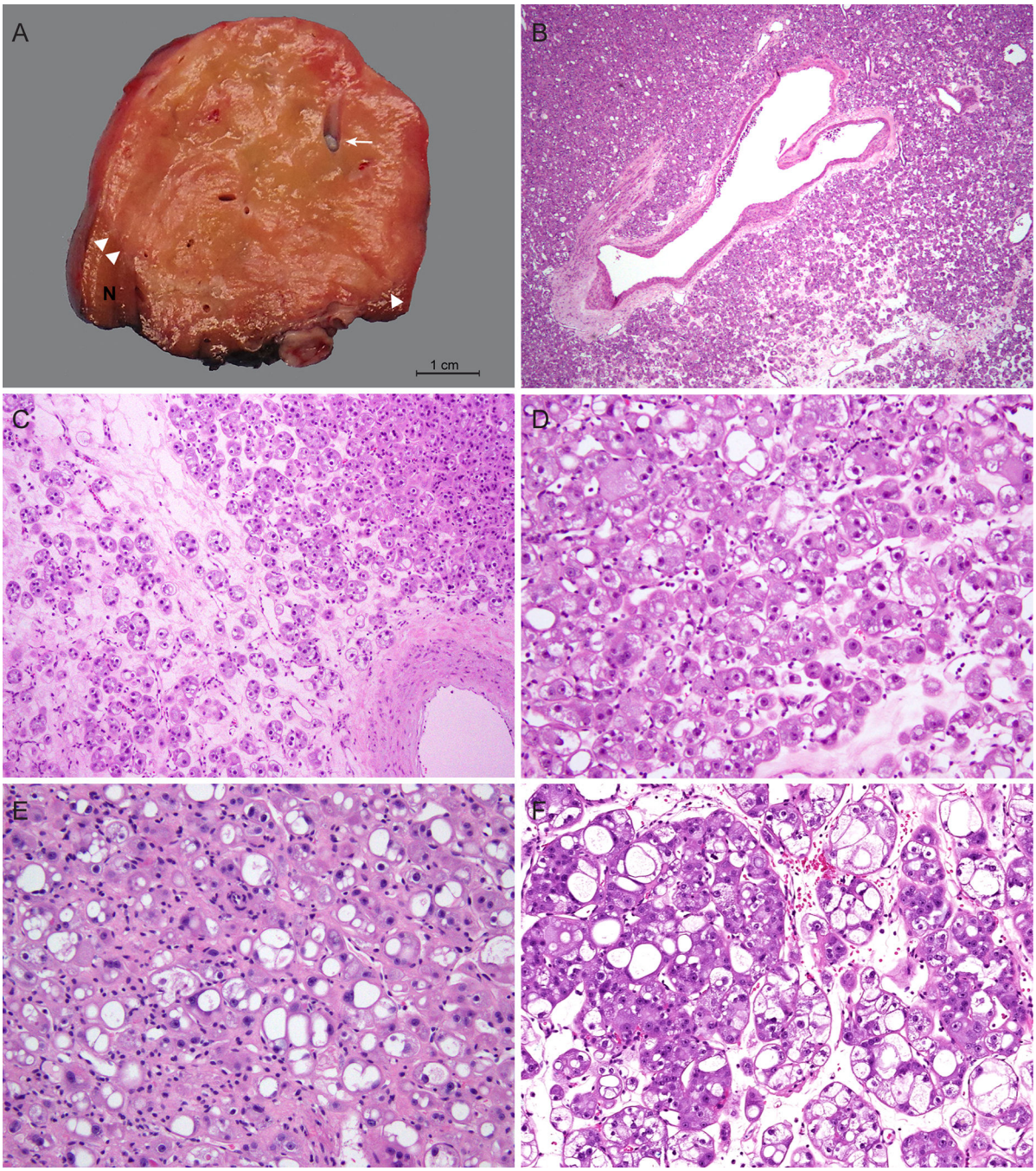

Figure 1.

Macroscopic and microscopic features of a distinct group of RCC with eosinophilic and vacuolated cytoplasm. (A) Tumors are well-circumscribed with tan-yellow to tan-brown, mostly solid cut surfaces. Arrow marks intratumoral vessels with medium to large caliber; arrowheads mark the boundary between tumor and adjacent renal parenchyma. (B-C) Tumors consist of nests of eosinophilic cells in a hypocellular and often edematous stroma. Dispersed single or minute clusters of cells are also present. Note an absence of foamy histiocytes or lymphocytic infiltrates in the stroma. (D-F) Tumor cells show round nuclei

with conspicuous to prominent nucleoli and eosinophilic, granular and vacuolated cytoplasm. Vacuolization varies from numerous small intracytoplasmic vesicles to large spaces almost occupying the entire cytoplasm. (D) Case 1, (E) Case 4, (F) Case 6.

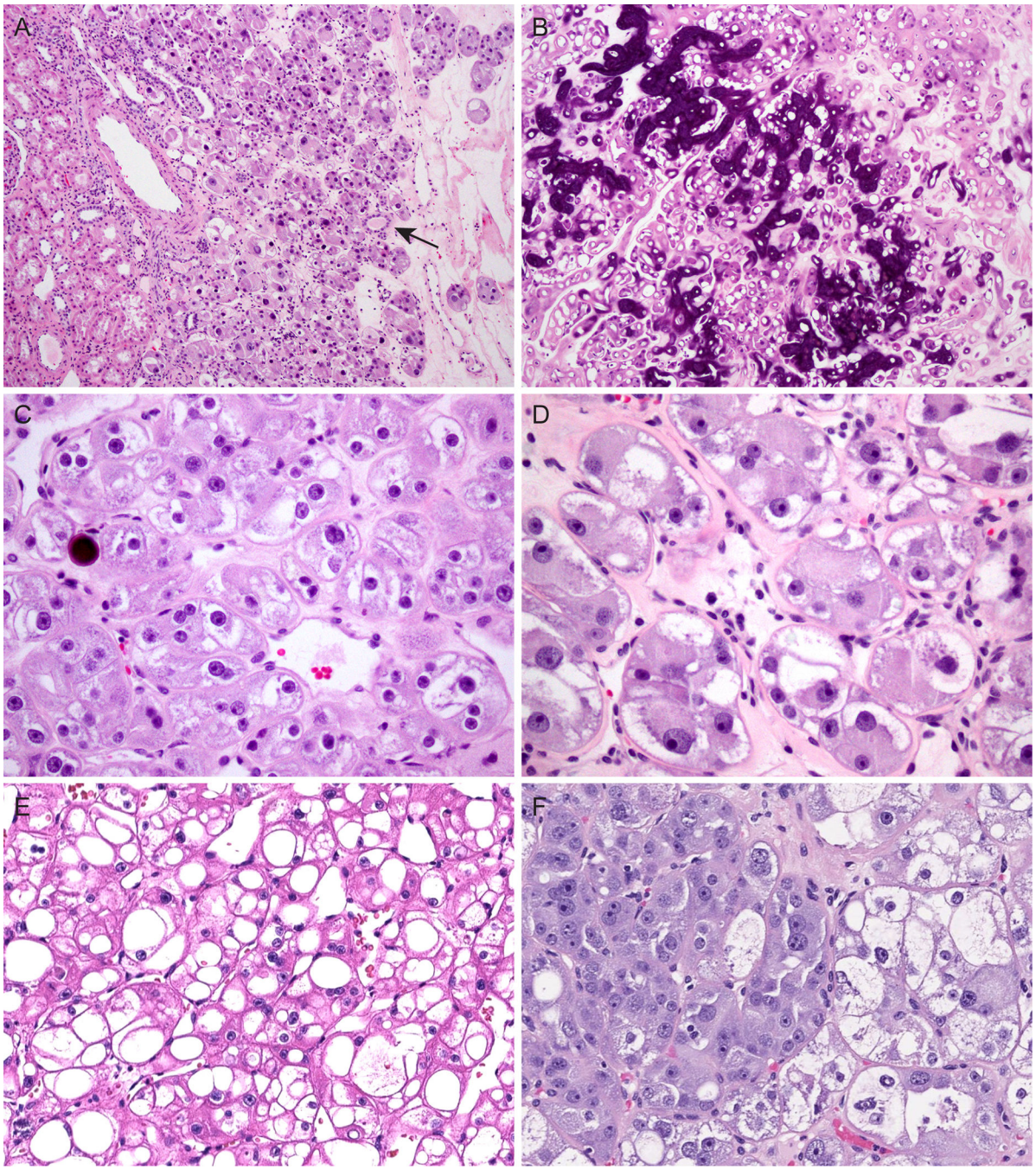

Figure 2.

Additional histologic features include: (A) lack of tumor capsule and entrapped renal tubules (arrow); (B) extensive calcifications; (C) microscopic calcifications and perinuclear cytoplasmic clearing, mimicking chromophobe RCC; (D) marked cytoplasmic eosinophilia with filamentous material and focal cytoplasmic stippling; (E) cribriform or sieve-like appearance in areas with tightly packed nests and extensive vacuolization; (F) abrupt transition between tumor cells with prominent vacuolization and those with dense, granular cytoplasm.

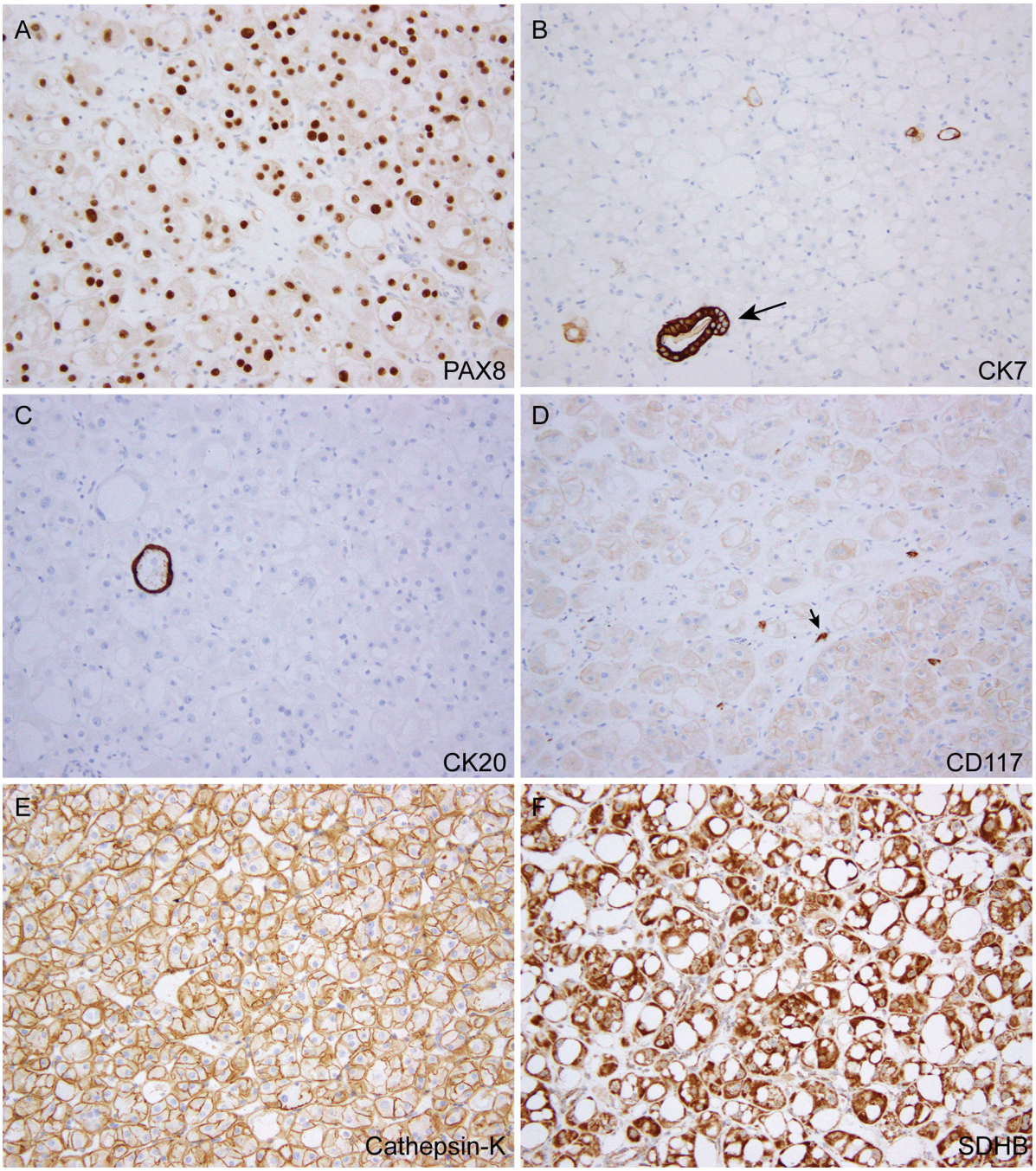

Figure 3.

Immunohistochemical features. (A) Positive nuclear staining for PAX8. (B-C) Tumor cells negative for CK7 (B) and CK20 (C) except for scattered rare cells/vacuoles; arrow in (B) marks an entrapped renal tubule. (D) Weak membranous staining for CD117; arrow marks a mast cell. (E) Diffuse cathepsin-K immunoreactivity. (F) Retained SDHB expression.

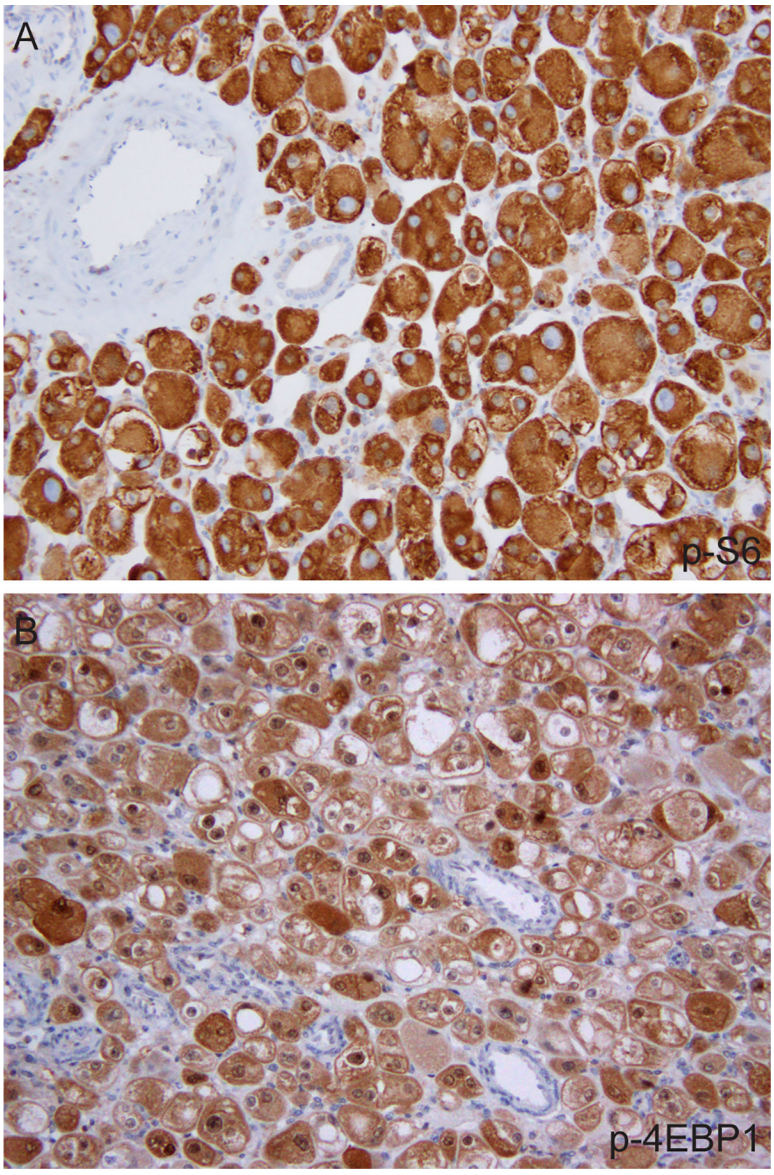

Figure 4.
Representative images of p-S6 (A) and p-4EBP1 (B) immunostains.

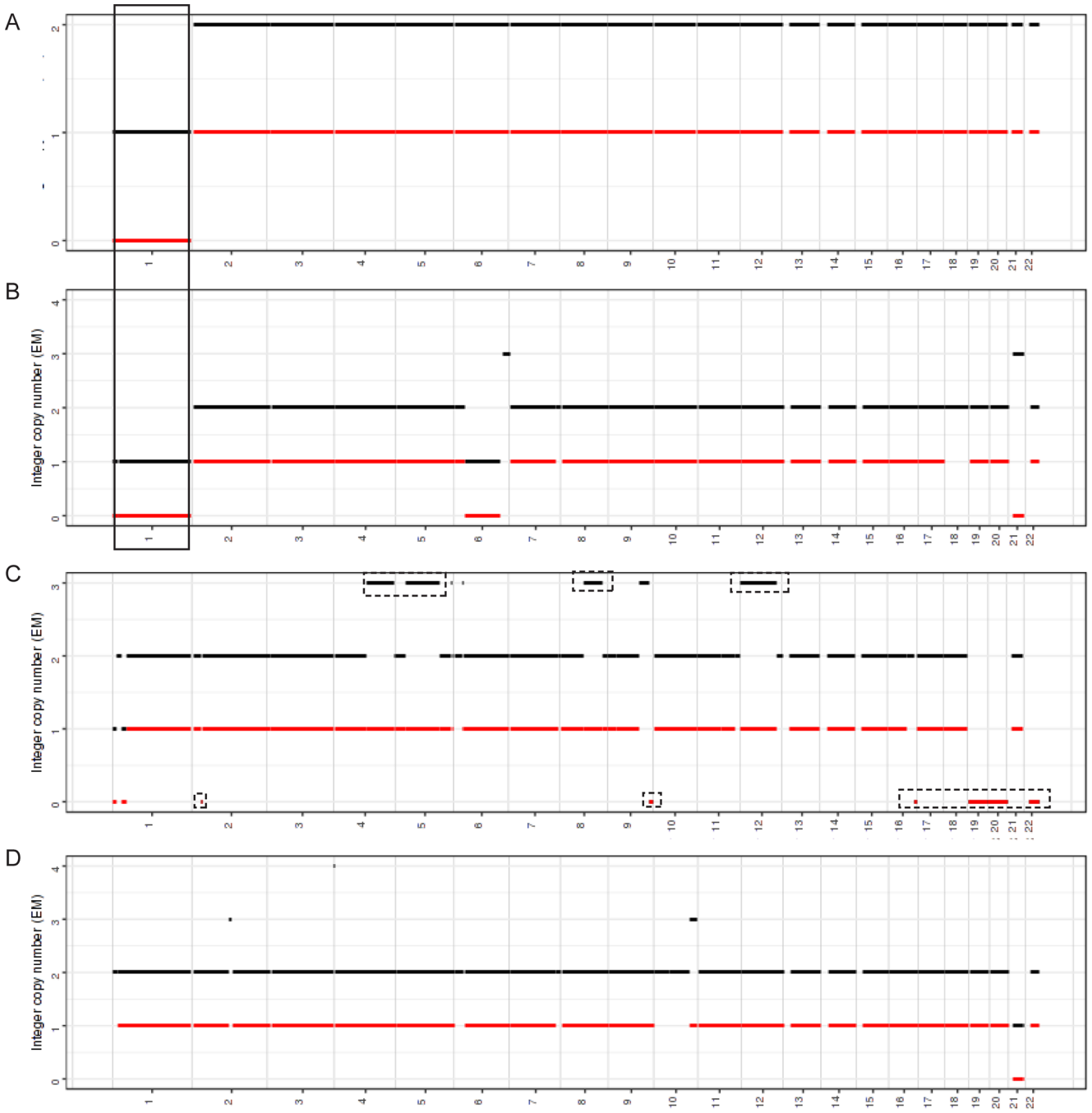

Figure 5.

FACETS analysis in 4 cases. The integer copy number (copy number call corrected for tumor purity and ploidy) is plotted on the y-axis. Diploid corresponds to n = 2. Chromosomes 1–22 are plotted on the x-axis. Black line - total copy number, red line - minor allele. (A-B) Cases 4 (A) and 5 (B) (*MTOR* p.L2427R) show recurrent chromosome 1 loss (solid box). (C-D) Cases 2 (C) and 6 (D) (biallelic *TSC2* mutations) have no shared

gains/losses. Dashed boxes in (C) mark copy number changes detected in minor clone(s) with an estimated clone fraction ≤ 9%.

Table 1.

Clinicopathologic characteristics of 7 cases in the cohort.

Pt	Age/Sex	Presentation	Imaging	Personal/Family history*	Size (cm)	pT	Growth pattern	Nuclei	Cytoplasm vacuolization	Thick-walled vessels	Calc	Foamy histiocytes/ lymphocytes	F/U (mo)
1	55/F	Incidental	R/solitary	None/None	2.5	pT1a	Nested, with dispersed single cells	Prominent nucleoli, multinucleation	Extreme	Yes	Yes	No	NED (128)
2	40/F	Incidental	R/solitary	None/None	5	pT1b	Nested, with dispersed single cells	Prominent nucleoli, multinucleation	Extreme	Yes	Yes	No	NED (21)
3	40/M	Right flank pain and urinary frequency	L/solitary	None/None	2.5	pT1a	Nested, with dispersed single cells	Prominent nucleoli, multinucleation	Extreme	Yes	No	No	NED (14)
4	68/F	UTI	L/solitary	Osteoporosis / None	4.4	pT1b	Nested, with dispersed single cells	Prominent nucleoli, multinucleation	Extreme	Yes	Yes, extensive	No	NED (13)
5	59/M	UTI	R/solitary, One simple cyst (2.3cm)	Hypertension / None	3.6	pT1a	Nested, with dispersed single cells	Prominent nucleoli, multinucleation	Extreme	Yes	Yes	No	NED (10)
6	52/M	Trauma	R/solitary	Trauma/NA	1.5	pT1a	Nested, with dispersed single cells	Prominent nucleoli, multinucleation	Extreme	Yes	No	No	NA
7	62/F	Incidental	R/solitary	NA	4.2	pT1b	Nested, with dispersed single cells	Prominent nucleoli, multinucleation	Extreme	Yes	No	No	NA

R, right; L, left; Calc, calcifications; F/U, follow-up; NA, not available; NED, no evidence of disease; UTI, urinary tract infection.

*History includes any past medical history (PMH) raising concerns for tuberous sclerosis complex (TSC), other significant PMH, and family history of renal cancer or any syndromic condition.

Table 2.

Immunohistochemical results and molecular alterations detected.

Pt	Immunohistochemistry												Somatic Mutations†	Copy Number Alterations
	PAX8	CK7	CK20	CD117	Cathepsin K	SDHB	FH	TFE3	HMB45	Melan A	pS6‡	p4EBP1‡		
1	**(+)**	**(−)**	**(−)**	**(−)**	**(+)**	**R**	**R**	**(−)**	**(−)**	**(−)**	**300**	**300**	**TSC2 p.R1138***	**ND**
2	(+)	(−)	(−)	Weak (+)	(+)	R	R	(−)	(−)	(−)	300	300	**TSC2 p.X373_splice** **TSC2 p.Q510Sfs***	Focal losses 1p36.3, 1p35; Focal gains 5q35, 6p22, 9q31-34; ¶Minor clone(s) with gains of 4q, 5, 8q, 12
3	(+)	(−)	(−)	Weak (+)	(−)	R	R	(−)	(−)	(−)	300	300	ND	ND
4	(+)	(−)	(−)	(−)	(+)	R	R	(−)	(−)	(−)	300	300	**MTOR p.L2427R**	Loss of 1
5	(+)	(−)	NA	Weak (+)	NA	R	R	(−)	(−)	(−)	NA	NA	**MTOR p.L2427R** NOTCH2 p.D1306N (VUS)#	Loss of 1; Loss of 6p-q24; LOH and gain of 21; Gain of 6q25-26
6	(+)	NA	(−)	(−)	(+)	R	R	(−)	NA	NA	300	230	**TSC2 p.X534_splice** **TSC2 p.K506Sfs*** PTPRD p.T988S (VUS)#	Loss of 21q; Focal gain 10q25-26
7	(+)	(−)	(−)	Weak (+)	focal (+)	R	R	(−)	(−)	(−)	250	230	ND	ND

LOH, loss of heterozygosity; R, retained; NA, not available; ND, not determined; VUS, variant of unknown significance.

‡Immunohistochemical stain result is shown in H-scores [H= intensity (0–3) x percentage of positive cells (1–100)].

†Mutations with known or likely oncogenic significance are marked in bold fonts.

#On the basis of variant allele frequency, the possibility of this VUS represents a germline single nucleotide polymorphism (SNP) cannot be excluded.

¶The estimated minor clone fraction is about 9%.